



# Detecting Sedimentary Cycles using Autocorrelation of Grain size

SUBJECT AREAS:  
GEOMORPHOLOGY  
PALAEOCLIMATE  
ATTRIBUTION  
GEOLOGY

Shangbin Xiao<sup>1,2</sup>, Rui Li<sup>1</sup> & Muhong Chen<sup>2</sup>

<sup>1</sup>China Three Gorges University, Yichang 443002, China, <sup>2</sup>South China Sea Institute of Oceanology, Chinese Academy of Sciences, Guangzhou 510301, China.

Received  
2 December 2012  
Accepted  
8 March 2013  
Published  
11 April 2013

Correspondence and requests for materials should be addressed to S.B.X. (shangbinx@163.com)

Detection of sedimentary cycles is difficult in fine-grained or homogenous sediments but is a prerequisite for the interpretation of depositional environments. Here we use a new autocorrelation analysis to detect cycles in a homogenous sediment core, E602, from the northern shelf of the South China Sea. Autocorrelation coefficients were calculated for different mean grain sizes at various depths. The results show that sediments derived from rapid depositional events have a better autocorrelation. Analysis of two other cores confirms this result. Cores composed of sediments deposited quickly under stable and/or gradually changing hydrodynamic conditions, have higher autocorrelation coefficients, whereas, those composed of sediments deposited during calm periods have relatively low autocorrelation coefficients. It shows that abrupt changes in autocorrelation coefficients usually indicate the existence of a boundary between adjacent sedimentary cycles, with each cycle beginning with a high positive autocorrelation coefficient of grain size and ending with a low negative one.

The detection of sedimentary cycles in cores is key to understanding their depositional environments, and determining if such data can be used to reconstruct high-resolution palaeoclimatic records. Sedimentary cycles are commonly identified using qualitative assessments of changes in, for example, grain size, sedimentary structure, and the stacked patterns of the sedimentary layers<sup>1–8</sup>. However, the precise identification of sedimentary cycles can sometimes be rather difficult, especially within relatively homogeneous sediments<sup>4,9,10</sup>. For example, Core NS97-13, a sedimentary sample collected from the South China Sea at a water depth of 2120 m (8°20.38'N, 115°55.38'E), is lithologically homogeneous and composed of mud<sup>11</sup>. Analysis of the anisotropy of the magnetic susceptibility and the results of AMS<sup>14</sup>C dating indicate that the sediments may have been deposited from turbidity currents. However, it is very difficult to identify any sedimentary cycles within the core, either visually or by measuring and analysing the grain size. This is a common problem specifically noted in other studies<sup>9,10,12,13</sup>.

Correlation is a mathematical tool frequently used in signal processing for analysing functions or series of values, and it describes the mutual relationship between two or more random variables. Autocorrelation describes the correlation of a set of data with itself<sup>4,15</sup>. This is not the same as cross-correlation, which is the correlation between two different signals<sup>14</sup>. A time-series data set can be separated into three components, namely the overall trend, the noise, and the cyclicity. Many researchers are interested in removing the trend and use autocorrelation to reveal important information about the temporal behaviour of the system. Autocorrelation may be also pervasive in sedimentary profiles<sup>16,17</sup>, and has been used between pixels in digital sediment images to measure average grain-size<sup>16,18–21</sup>.

In the present study, we analyze Core E602, a sample collected from the shelf of the northern South China Sea (Fig. 1), develop a new mathematical method that involves the autocorrelation analysis of the grain size and discuss the mechanisms of sediments transportation involved. Our new method enables the detection of sedimentary cycles within any core, but within lithologically homogeneous cores in particular. Moreover, the method is quantitative and eliminates subjective interpretation that can be difficult to replicate between investigators and studies.

## Results

Core E602 has two lithostratigraphic units determined by changes in lithology and color (Fig. 2). The lower unit (37 to 368 cm) is composed of dark-gray silty sand and is homogeneous with little variation in sand, silt and clay content. The upper unit (0 to 37 cm) changes gradually up-core from silty-sand to sandy-silt. The clay content also appears to increase gradually in the same direction.

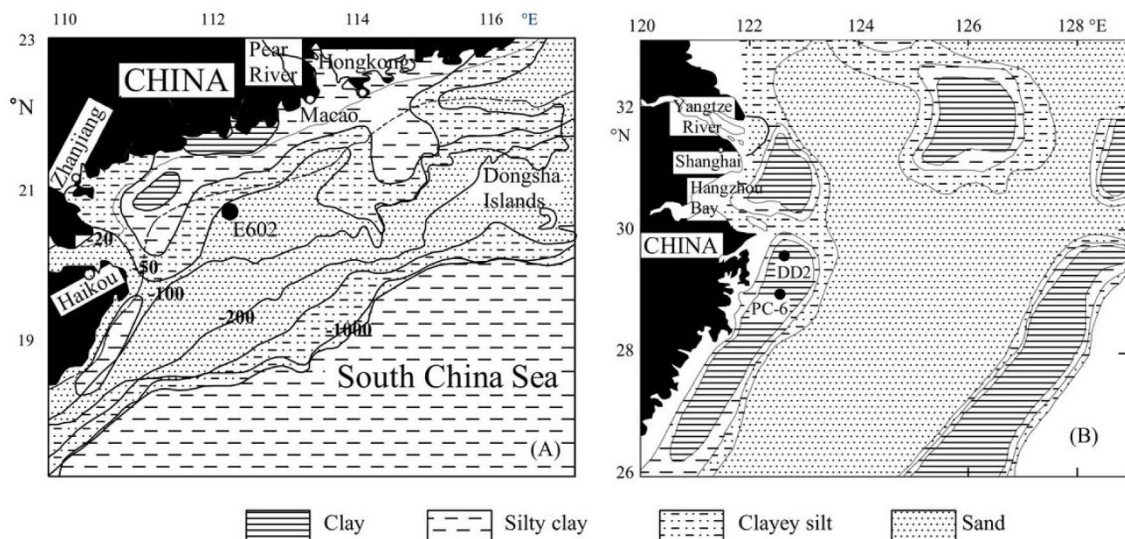


**Figure 1** | Location of Cores E602 (A) and DD2 and PC-6 (B). Maps of sediment distribution (A) and (B) are reproduced from Liu et al.<sup>36</sup> and Qin et al.<sup>37</sup>, respectively.

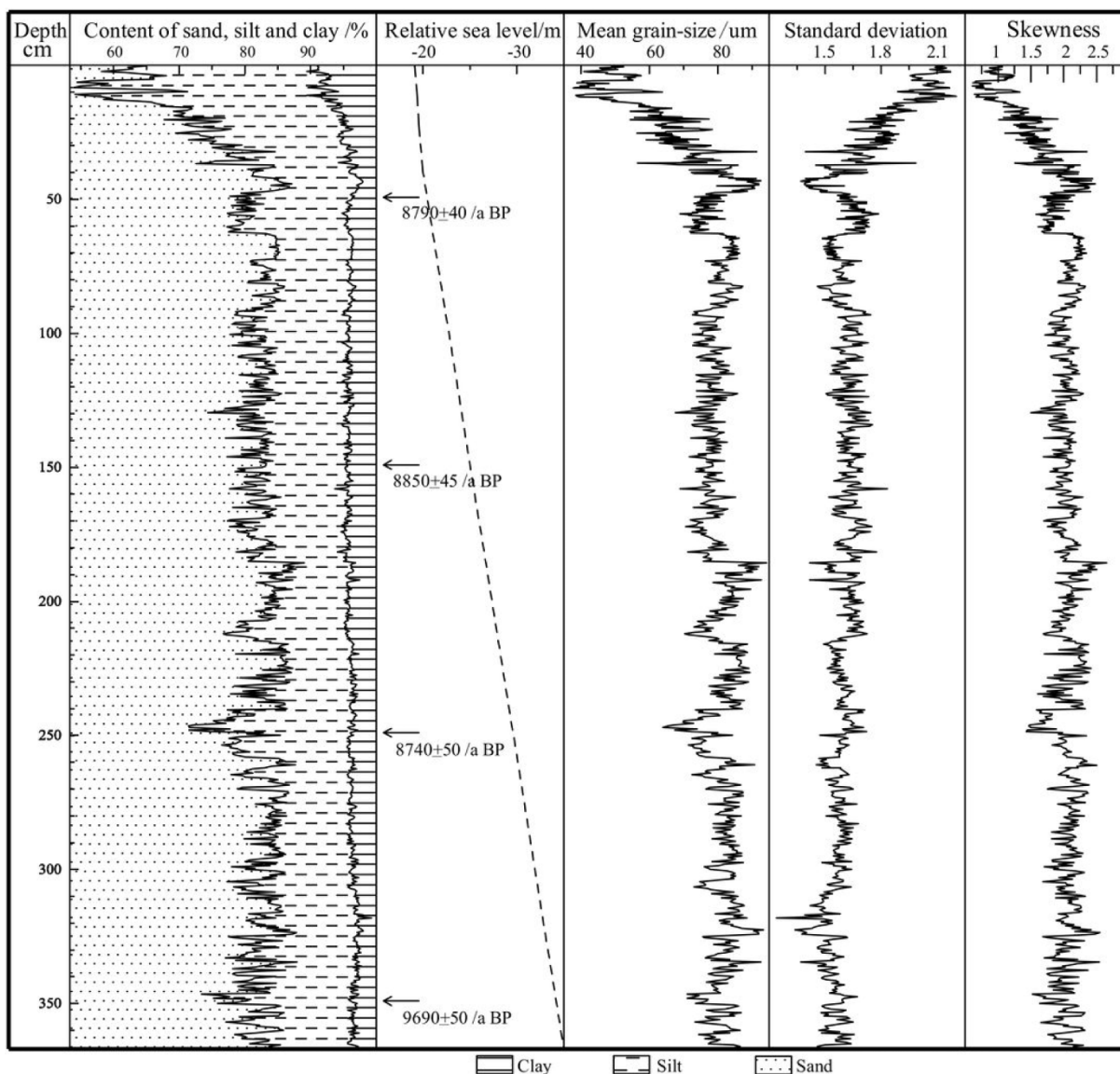


**Figure 2** | Grain size, chronology, and granulometry of Core E60.

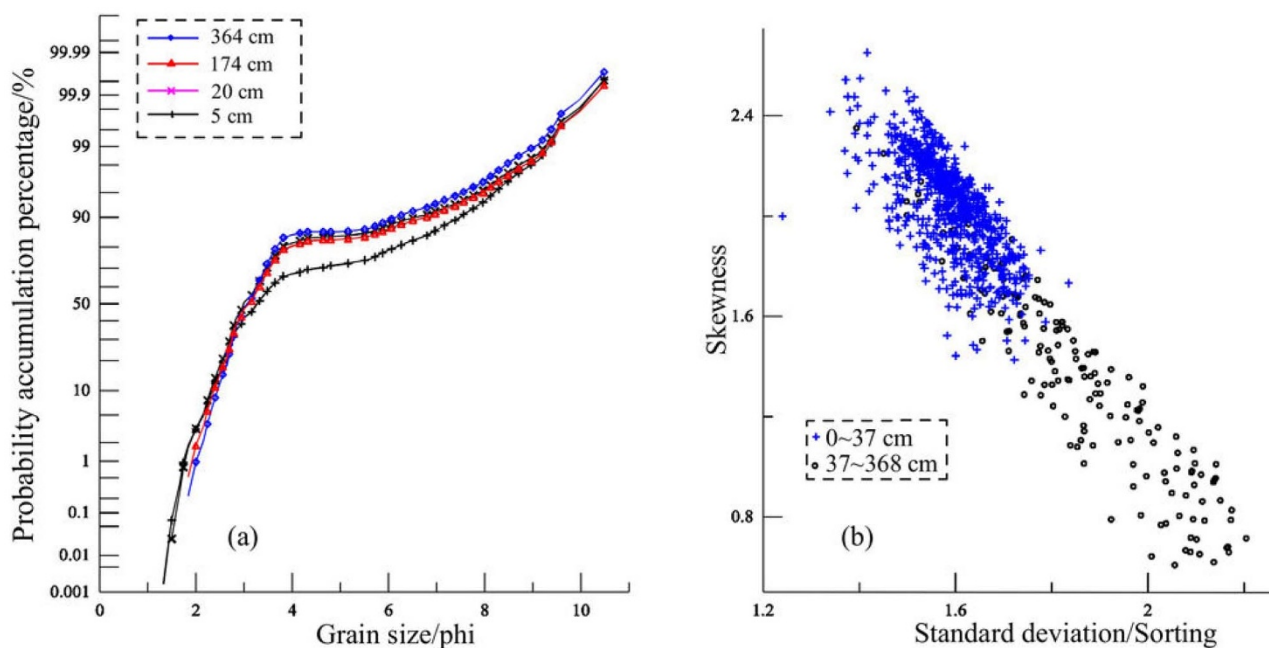


**Figure 3** | Distribution of accumulation probability (a) and skewness vs. standard deviation of grain size distribution (b) for Core E602.

As shown in Fig. 3(a), all of the 886 sediment samples from Core E602 are composed of saltation and suspension fractions, the boundary of which is located at approximately 3.8 PHI. The suspension fraction ranges in content from 15 to 35%. The slope of the saltation fraction, which reflects a sorting trend, remains almost the same throughout both core units.

The standard deviation of grain-size distributions of the sediment samples obtained from the lower core unit ranges from 1.3 to 1.6, and their skewness ranges from 1.4 to 2.5. Samples obtained from the upper unit exhibit little change in sediment sorting, with standard deviations in the range 1.6–2.2. However, the skewness of grain-size distributions of the samples decreases to 0.6 to 1.6, perhaps as a result of the higher fine-sediment fraction in the upper unit. Given that the bimodal frequency curves shown in Fig. 4 are typical of grain-size distributions for all the samples from the core, the higher content of fine sediment fraction did not obviously affect sediment sorting in the samples, but did result in a reduced degree of the skewness.

The CM patterns in core sediments (Fig. 5(a)) plotted on the QR segment, which represents graded suspension, and the RS segment, which represents uniform suspension<sup>22,23</sup> (Fig. 6(b)). The QR

segment dominated the CM patterns for the lower unit, whereas the RS segment was episodic. The RS segment determined the CM patterns for the upper unit, which implies that a uniform suspension during the deposition of the unit was controlled by traction currents (Fig. 7). Furthermore, all of the sediment samples fall within a small region in the CM plot (Fig. 5a), which indicates that they are well sorted. It has already been noted that the upper unit of core E602 exhibits an increase in fines sediment from top to bottom, as well as decreases in grain-size and sorting. However, also evident from the CM plot (Fig. 5b) are the relatively larger C values of sediment from 0–25 cm depth, signifying that the sediments are coarser, than those obtained from below 25 cm.

The foraminifera samples at the base of core E602 (348–350 cm) gave a <sup>14</sup>C age of 10289–10584 a BP (Table 1), which suggests that the deposition began during the early Holocene. According to a recent report on sea level changes in the South China Sea<sup>24</sup>, sea level rose from approximately –35 m to –20 m during this period (~10 to ~9 ka BP). Combining water depth at the coring site, and the core length therefore gives a paleowater depth of ~30–45 m, placing it within the shallow continental shelf environment.

The uniform content of sand, silt and clay, and granulometry in the lower unit of E602, implies reworking of late Pleistocene sediments composed of medium and fine sand with high textural maturity. By contrast, fine-grained terrigenous sediment dominates the upper unit, with the coarsest sediment being deposited at the top of the core (Fig. 5b).

The characteristics of Core E602, in terms of grain size, sedimentary structure (Fig. 7b) and CM patterns, indicate that its sediments were, for the most part, deposited under stormy conditions, which is consistent with the modern reports of frequent tropical storms<sup>25</sup>. Resuspension occurs when deep water waves enter water shallower than one-half the wave length (i.e. the wave base)<sup>26</sup>. The wave base under a fair-weather is less than 10–15 m<sup>27</sup>. However, the storm deposit extends about 40 m<sup>13</sup>, i.e., bottom sediments below the fair-weather wave base would be reworked under storm condition<sup>27</sup>. Given that each storm can gradually strengthen, reduce, or maintain its intensity, means that it could produce sedimentary units with decreasing (segment (21) in Figure 8), increasing (segment (9) in Figure 8), or invariable mean sediment-size with depth respectively.

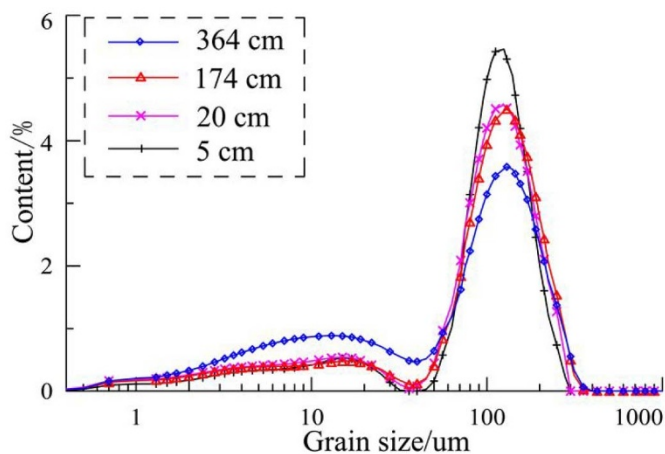


**Figure 4** | Grain size distribution of several samples obtained from Core E602.



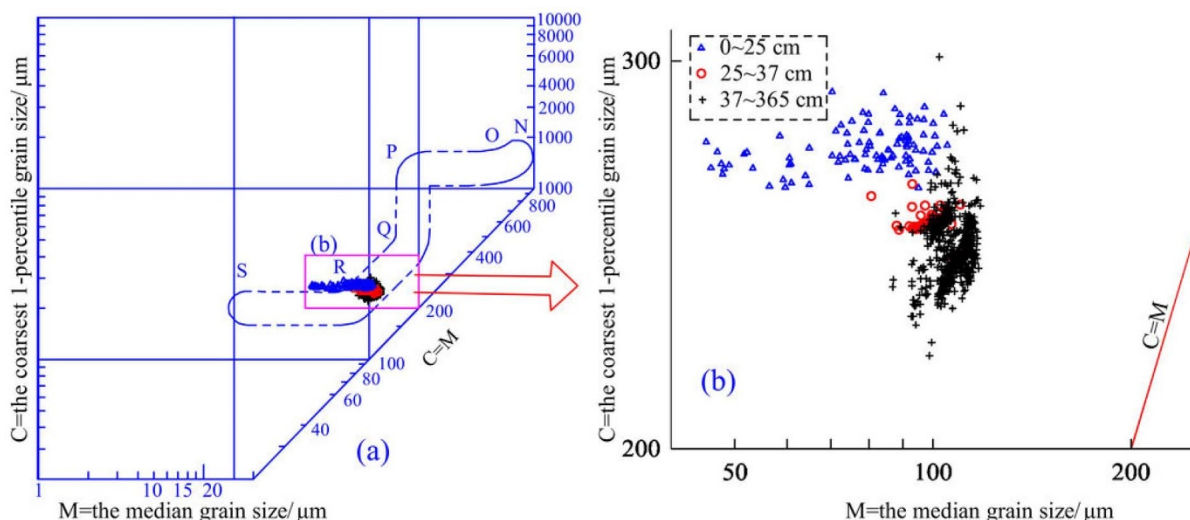


**Figure 5 | CM plots of Core E602.** Passega’s CM image technique, where  $C$  is the coarsest one percentile (the value at 99% on a cumulative curve) and  $M$  is the median grain-size, has been widely used to relate the grain-size characteristics of sediments to the processes of their deposition. Passega<sup>23,34</sup> and Passega & Byramjee<sup>35</sup> made a distinction between the following types of sediment movement: (1) particles rolled on the bed, even when there is no turbulence. (2) Graded suspension (the term is preferred to ‘saltation’), composed of sand and coarseness decrease from the bottom of the river to an elevation of 2 m upwards. The size of the coarsest particles in the graded suspension ( $C_s$ ) fluctuates according to the maximum turbulence when settling begins. (3) Overlying graded suspension, Passega described uniform suspension, defined by a constant concentration of particles at the top of the water column. Uniform suspension may be in direct contact with the bed when turbulence decreases below a threshold, allowing the graded suspension to settle on the bed. Slow-flowing rivers display uniform suspension, even during floods<sup>22</sup>.

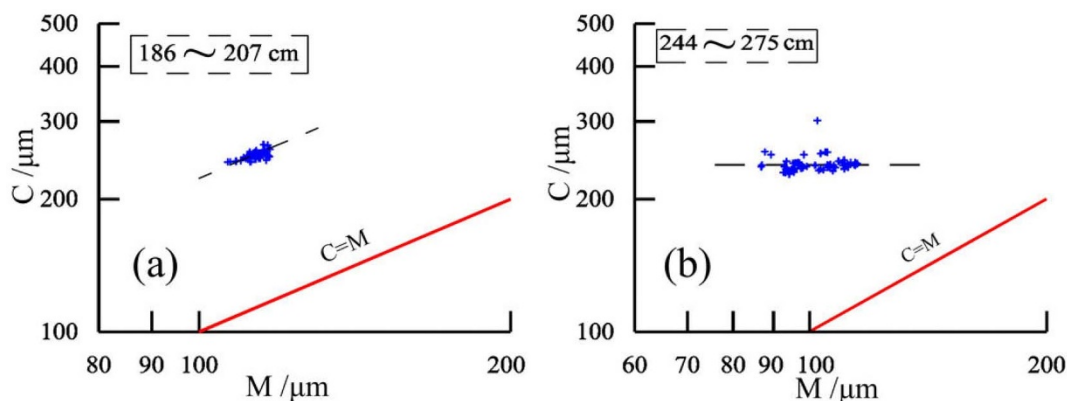


**Figure 6 | Different CM patterns within Core E602.**

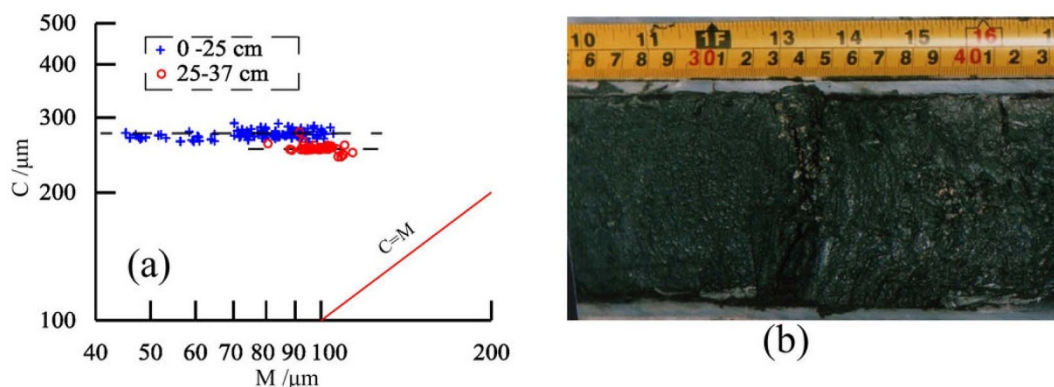


**Figure 7 | CM plot of the upper unit of Core E602 (a) and a typical sedimentary pattern resulting from a storm current (b).**

Table 1 | AMS  $^{14}\text{C}$  data of Core E602

Depth(cm)	Material	$^{14}\text{C}$ age/a BP	Calendar age/a BP	
			(1 sigma)	(2 sigma)
48~50	<i>Nummulites</i>	$8790 \pm 40$	9068~9597	9019~9756
148~150		$8850 \pm 45$	9097~9742	9050~9807
248~250		$8740 \pm 50$	9038~9576	8988~9751
348~350	<i>Nummulites, Pseudorotaria, Elphidium</i>	$9690 \pm 50$	10289~10584	10201~11119

First-order autocorrelation coefficients of mean grain-size vary with sample size (5–30) at different depths, as shown in Figure 8. Autocorrelation coefficients vary considerably at some depths, for example from  $-0.59$  to  $0.50$  at  $\sim 27$  cm, but change little at other depths, for example at  $\sim 70$  cm. Figure 9 illustrates how the points of abrupt change in autocorrelation coefficient fit remarkably well with changes in mean grain-size of the sediment samples.

## Discussion

The accumulation of sediment can be either rapid, for example during storms as a result of turbidity currents, or it can be much slower during

periods of calm weather. Assuming sediment provenance is invariable and water depth does not change, calm hydrodynamic conditions produce little variation in grain size, and thus no abrupt changes in the autocorrelation coefficients of mean grain-size. However, storms or tsunamis can alter the hydrodynamic conditions considerably, and can cause rapid accumulation of sediment with significant changes in grain size<sup>1,4,8</sup>. A sedimentary cycle may be formed during a single storm event, and depending on changes in current intensity, can result in either a graded or ungraded sequence. Thus, although there are sometimes no discernable changes in grain size within a particular sequence of storms, the degree of autocorrelation may be high due to the inertia

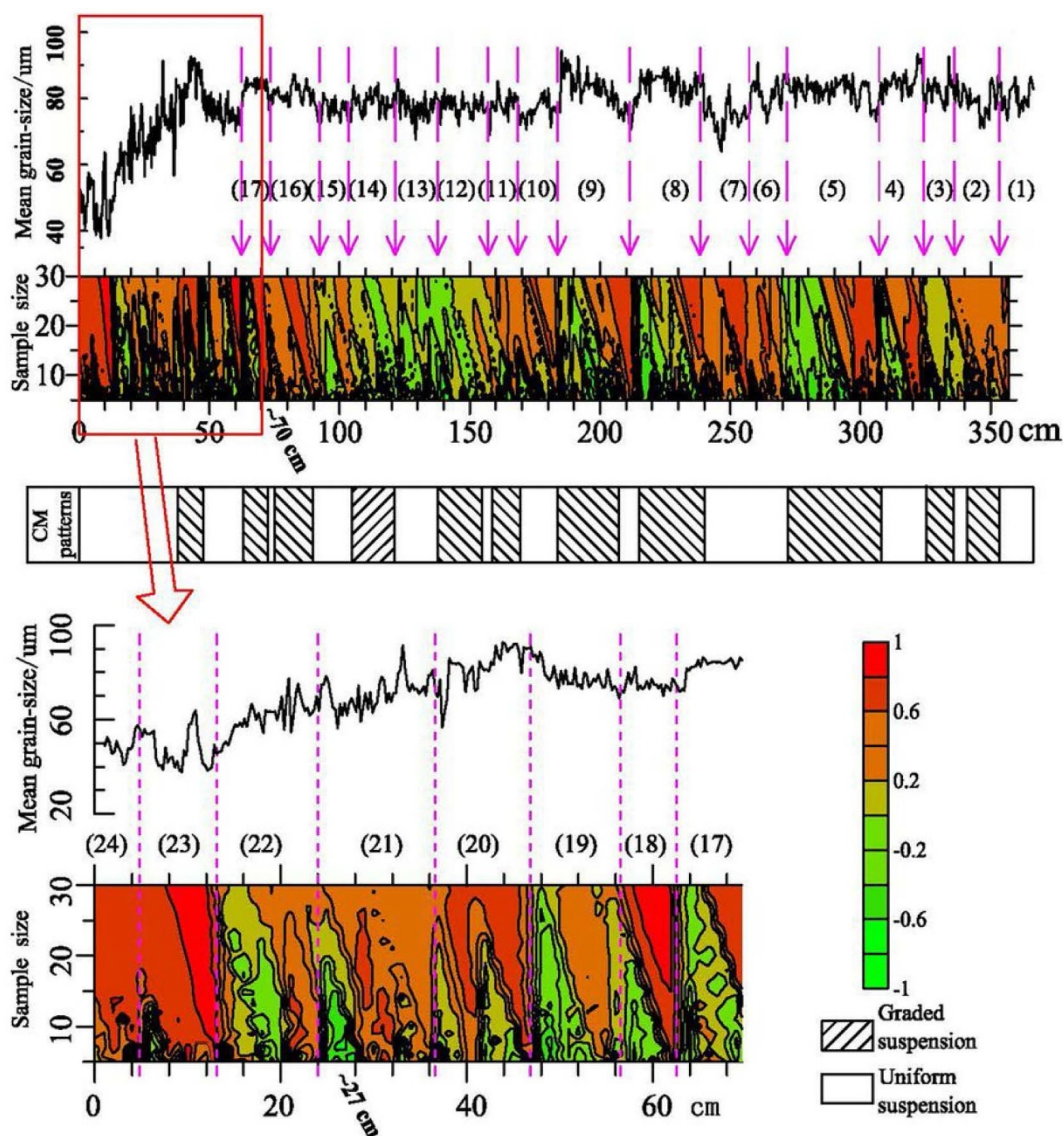
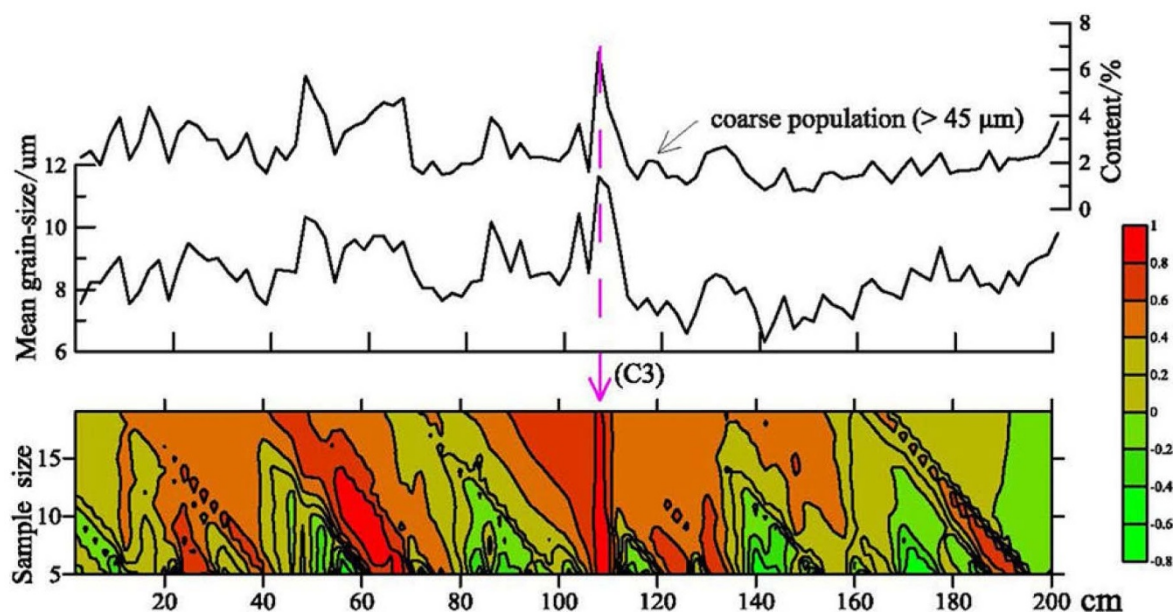


Figure 8 | Variation in the first-order autocorrelation coefficients of mean grain-size with sample size for Core E602. The numbers 1–24 in parentheses refer to different sedimentary layers/cycles.



**Figure 9** | Variation in the first-order autocorrelation coefficients of mean grain-size with sample size for Core DD2. A vertical abrupt change (C3, which recorded a storm event) in the gradient of the contour of autocorrelation coefficients of the core is indicated by an arrow.

or internal coherence that is inherent in the rapid accumulation of sediment. Figure 8 shows that sharp changes in autocorrelation coefficient tend to be found at the boundaries between different cycles that may have resulted from large differences in the energy of successive storm currents.

In addition to storm cessation, a sediment cycle could terminate for several other reasons, including abrupt changes in water depth or sediment supply<sup>4,8,28</sup>. However, in the studies cores, relatively rapid sediment accumulation or more stable sedimentation occurs at the

base of a new cycle, which results in a high degree of autocorrelation of grain size. This may in turn result in a degree of inertia of grain size within a sedimentary profile. Thus, a cycle begins with high positive values of autocorrelation coefficient and ends with low negative ones. It is this inertia that allows the application of the autocorrelation analysis of grain size to the determination of sedimentary cycles in cores of this type.

It is relatively easy to identify sedimentary sequences or cycles those are composed of individual layers that are either normally

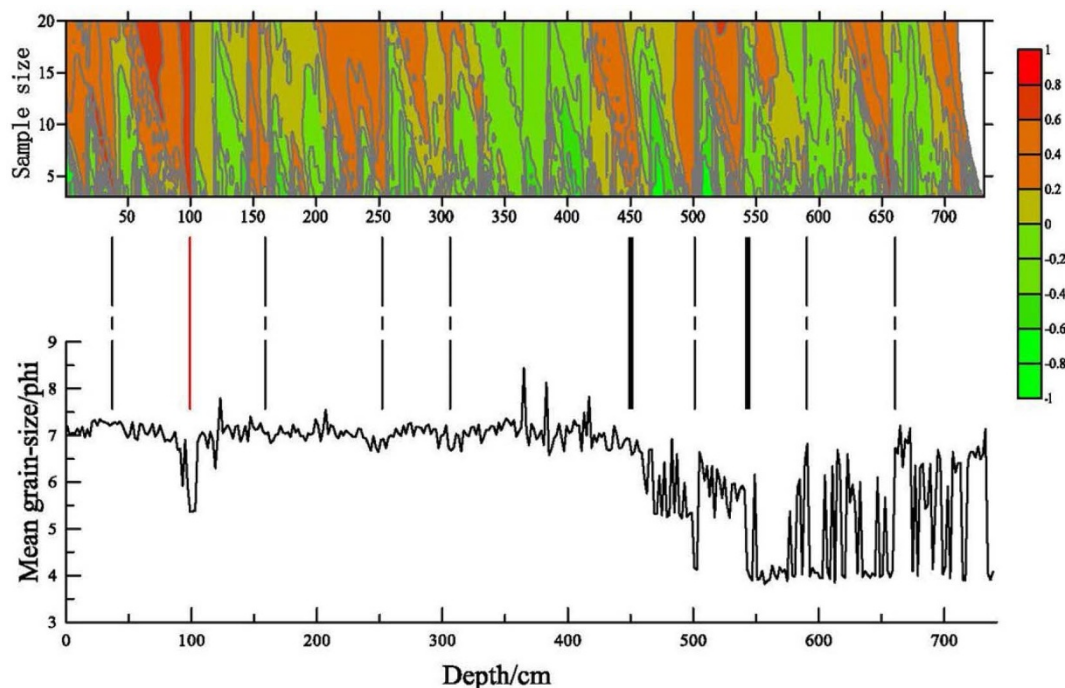


**Figure 10** | Variation in first-order autocorrelation coefficients of mean grain-size with sample size for Core PC-6. The two black bold vertical lines indicate the boundaries of neighbouring cycles; multiple black dot-dashed lines indicate the boundaries of neighbouring subcycles; and the red vertical line, which shows an abrupt change in the gradients of the contour of the autocorrelation coefficients of the core, indicates the base of a storm layer. Note that no obvious subcycles of sedimentation can be discerned in the muddy unit above 450 cm using traditional sedimentological methods.





graded (Layers 19 & 20 in Fig. 8) or reverse-graded (Layers 8 & 9 in Fig. 8), because any abrupt changes in grain size at the boundaries between these layers are clear. However, in some cases there are no clear changes in grain size within a sequence that is composed of sediments deposited during a number of different events (e.g. Layers 10~13 & 17~18 in Fig. 8). Under such circumstances, it is difficult to determine the number of sedimentary cycles with any accuracy. In Core E602, for example, the small variation in mean grain-size values from ~183 to ~100 cm (Layers 10~13 in Fig. 8) formed a cycle of sedimentation, similar to an aggradational stack. It was difficult to identify the sedimentary cycles or sequences of the core in terms of changes in mean grain-size alone. Fortunately, autocorrelation analysis can reveal the hidden relationships that affect sediments at different depths. Abrupt changes in autocorrelation coefficient of grain size can provide a clear indication of the boundaries between neighbouring sedimentary layers. For example, at least 24 depositional cycles have been identified in Core E602 (Fig. 8).

In a further example, the muddy unit of Core DD2 was formed in a relatively stable sedimentary environment and during a period of calm weather<sup>29</sup>. However, the sediments at ~107 cm in the core (C3 on Fig. 9) may be the result of the combined influence of a winter coastal current and a storm current, because there is also an abrupt change in the autocorrelation coefficients of the core at this point.

Core PC-6 provides a third example (Fig. 10). In this core, sediments deposited during different environmental conditions appear to have different characteristics of grain size and stacked patterns. Abrupt changes in the autocorrelation coefficients of the core occurred not only at these boundaries, but also at the boundaries of the subcycles of sedimentation. The latter are sometimes difficult to identify within relatively homogeneous sedimentary profiles. At the same time, the storm deposit event reported at ~100 cm<sup>30</sup> is clearly revealed by the abrupt change in the autocorrelation coefficients of grain size within the core (Fig. 10).

A degree of autocorrelation in sedimentary profiles is a widespread phenomenon, and is a result of the similarity of the hydrodynamic conditions present in the stable sedimentary environment that characterized the sedimentation<sup>31</sup>. Sediments derived from storms or other events have a higher degree of autocorrelation as a result of their rapid deposition<sup>8</sup>, and abrupt changes in autocorrelation coefficient usually indicate the boundaries between successive sedimentary cycles. The analysis of autocorrelation coefficients is therefore a useful tool in the identification of sedimentary sequences or cycles, and our results confirm its potential of for detecting sedimentary cycles in homogeneous sediment sequences. Combined with the use of rapid techniques<sup>16,18–21</sup> to determine grain-size from digital sediment images, autocorrelation analysis should therefore improve the accuracy of sedimentary environmental determination.

## Methods

Core E602, with a length of 3.68 m, was collected with gravity sampling pipe in October 2004 from a sandy area on the northern shelf of the South China Sea (112°14.88'E, 20°44.93'N), in a water depth of 65 m, and distant from any estuarine influence. In the laboratory, the core was described in detail and then split into a total of 886 samples (300 samples at 0.25 cm intervals from 0 to 75 cm and 586 samples at 0.5 cm intervals from 75 to 368 cm). The samples were initially pre-processed by the addition of excess H<sub>2</sub>O<sub>2</sub> ( $\varphi = 30\%$ ), followed by the addition of HCl (3N). The distribution of grain size was classified following Wentworth<sup>32</sup>, and measured using a Mastersizer 2000 from Malvern Instruments Ltd., with a range of measurement of 0.02 to 2000  $\mu\text{m}$  and a resolution of 0.01 PHI. The errors in mean grain size for the same sample obtained following repeated measurements were less than 3%. The mean grain size (unit: PHI) was used to calculate the autocorrelation coefficients of the grain size data.

Radiocarbon dating of the core sediments was carried out at the National Ocean Sciences Accelerator Mass Spectrometry Facility (NOSAMS), Woods Hole Oceanographic Institution. All the <sup>14</sup>C ages (Table 1) were calibrated to give calendar ages using CALIB4.3<sup>33</sup>.

The significance of the autocorrelation of grain size is herein discussed in the context of two other sedimentary cores obtained from the inner shelf of the East China Sea that have previously been described, namely DD2<sup>29</sup> and PC-6. Core DD2<sup>29</sup> is composed of muddy sediments formed in a shallow continental shelf. Core PC-6

shows a range of sedimentary dynamics associated with foreshore, nearshore and shallow continental shelf environments<sup>30</sup>.

As is known<sup>16</sup>, the correlation coefficient of a pair of random variables ( $X, Y$ ) is given by the formula:

$$r = \frac{\sum_{i=1}^n (x_i - \bar{x})(y_i - \bar{y})}{\sqrt{\sum_{i=1}^n (x_i - \bar{x})^2 \sum_{i=1}^n (y_i - \bar{y})^2}} \quad (1)$$

Where  $\bar{x}$  and  $\bar{y}$  are the average values of  $X$  and  $Y$ , respectively;

$X_i$  and  $Y_i$  are the  $i$ -th specific variable values of  $\{(x_i, y_i): i = 1, \dots, n\}$ ;

$i =$  a particular case  $i$ ;

$n =$  the number of cases.

The autocorrelation coefficient<sup>16</sup> of a series of data  $\{x_i: i = 1, \dots, n\}$ , is also calculated by the same formula above except  $y_i$  is replaced with  $x_{i+1}$  in a form lagged by one (i.e., first order autocorrelation) or with  $x_{i+k}$  in a form lagged by  $k$  (i.e.,  $k$  order autocorrelation).

Because the number of cases adopted has direct influence on the values of both the autocorrelation coefficient of the variable  $X$  and correlation coefficient of a pair variables ( $X, Y$ ), varying number of cases (range: 3~20) from a successive grain size data are taken here to calculate the autocorrelation coefficients and disclose their changes with depth.

- Kortekaas, S. & Dawson, A. Distinguishing tsunami and storm deposits: an example from Martinhal, SW Portugal. *Sedimentary Geology* **200**, 208–221 (2007).
- Horikawa, K. & Ito, M. Non-uniform across-shelf variations in thickness, grain size, and frequency of turbidites in a transgressive outer-shelf, the Middle Pleistocene Kakinokidai Formation, Boso Peninsula, Japan. *Sedimentary Geology* **220**, 105–115 (2009).
- González-Álvarez, R. *et al.* Paleoclimatic evolution of the Galician continental shelf (NW of Spain) during the last 3000 years: from a storm regime to present conditions. *Journal of Marine Systems* **54**, 245–260 (2005).
- Morton, R. A., Gelfenbaum, G. & Jaffe, B. E. Physical criteria for distinguishing sandy tsunami and storm deposits using modern examples. *Sedimentary Geology* **200**, 184–207 (2007).
- Sun, Y., Gao, S. & Li, J. Preliminary analysis of grain-size populations with environmentally sensitive terrigenous components in marginal sea setting. *Chinese Science Bulletin* **48**, 184–187 (2003).
- Anthony, E. J. & Héquette, A. The grain-size characterisation of coastal sand from the Somme estuary to Belgium: sediment sorting processes and mixing in a tide- and storm-dominated setting. *Sedimentary Geology* **202**, 369–382 (2007).
- Sedgwick, P. E. & Davis, R. A. Stratigraphy of washover deposits in Florida: implications for recognition in the stratigraphic record. *Marine geology* **200**, 31–48 (2003).
- Bentley, S. J., Sheremet, A. & Jaeger, J. M. Event sedimentation, bioturbation, and preserved sedimentary fabric: Field and model comparisons in three contrasting marine settings. *Continental Shelf Research* **26**, 2108–2124 (2006).
- Tuttle, M. P., Ruffman, A., Anderson, T. & Jeter, H. Distinguishing tsunami from storm deposits in eastern North America: the 1929 Grand Banks tsunami versus the 1991 Halloween storm. *Seismological Research Letters* **75**, 117–131 (2004).
- Dawson, A. G. & Shi, S. Tsunami deposits. *Pure and applied geophysics* **157**, 875–897 (2000).
- Tang, X., Chen, M., Liu, J., Zhang, L. & Chen, Z. The anisotropy of magnetic susceptibility of Core NS97-13 sediments from the Nansha Islands sea area in the southern South China Sea. *Acta Oceanologica Sinica* **31**, 69–76 (in Chinese with English Abstract) (2009).
- Allison, M. A., Sheremet, A., Goñi, M. A. & Stone, G. W. Storm layer deposition on the Mississippi–Atchafalaya subaqueous delta generated by Hurricane Lili in 2002. *Continental Shelf Research* **25**, 2213–2232 (2005).
- Goff, J., McFadgen, B. & Chagué-Goff, C. Sedimentary differences between the 2002 Easter storm and the 15th-century Okoropunga tsunami, southeastern North Island, New Zealand. *Marine geology* **204**, 235–250 (2004).
- Phillips, C., Parr, J. & Riskin, E. *Signals, Systems, and Transforms*. (Prentice Hall 1999).
- Herman, E. K., Toran, L. & White, W. B. Quantifying the place of karst aquifers in the groundwater to surface water continuum: A time series analysis study of storm behavior in Pennsylvania water resources. *Journal of Hydrology* **376**, 307–317 (2009).
- Rubin, D. M. A simple autocorrelation algorithm for determining grain size from digital images of sediment. *Journal of Sedimentary Research* **74**, 160–165 (2004).
- Xiao, S., Liu, W., Li, A., Yang, S. & Lai, Z. Pervasive autocorrelation of the chemical index of alteration in sedimentary profiles and its palaeoenvironmental implications. *Sedimentology* **57**, 670–676 (2009).
- Barnard, P., Rubin, D., Harney, J. & Mustain, N. Field test of an autocorrelation technique for determining grain size using a digital camera. *Sedimentary Geology* **201**, 180–195 (2007).
- Warrick, J. A. *et al.* Cobble Cam: Grain-size measurements of sand to boulder from digital photographs and autocorrelation analyses. *Earth Surface Processes and Landforms* **34**, 1811–1821 (2009).



20. Buscombe, D. & Masselink, G. Grain-size information from the statistical properties of digital images of sediment. *Sedimentology* **56**, 421–438 (2008).
21. Buscombe, D. Estimation of grain-size distributions and associated parameters from digital images of sediment. *Sedimentary Geology* **210**, 1–10 (2008).
22. Bravard, J.-P. & Peiry, J.-L. The CM pattern as a tool for the classification of alluvial suites and floodplains along the river continuum. *Geological Society, London, Special Publications* **163**, 259–268 (1999).
23. Passega, R. Grain size representation by CM patterns as a geologic tool. *Journal of Sedimentary Research* **34**, 830–847 (1964).
24. Hori, K. *et al.* Delta initiation and Holocene sea-level change: example from the Song Hong (Red River) delta, Vietnam. *Sedimentary Geology* **164**, 237–249 (2004).
25. Davies, J. *Geographical variation in coastal development*. (Longman Publishing Group, 1972).
26. Evans, R. D. Empirical evidence of the importance of sediment resuspension in lakes. *Hydrobiologia* **284**, 5–12 (1994).
27. Wright, M. E. & Walker, R. G. Cardium Formation (U. Cretaceous) at Seebe, Alberta-storm-transported sandstones and conglomerates in shallow marine depositional environments below fair-weather wave base. *Canadian Journal of Earth Sciences* **18**, 795–809 (1981).
28. Kakinoki, T., Tsujimoto, G., Yamada, F., Sakai, D. & Uno, K. Beach profile and sediment characteristics of a mixed sand beach under diurnal sea level variations. *Journal of Coastal Research* **SI 64**, 765–770 (2011).
29. Xiao, S. *et al.* Recent 2000-year geological records of mud in the inner shelf of the East China Sea and their climatic implications. *Chinese Science Bulletin* **50**, 466–471 (2005).
30. Xiao, S. *et al.* Coherence between solar activity and the East Asian winter monsoon variability in the past 8000 years from Yangtze River-derived mud in the East China Sea. *Palaeogeography, Palaeoclimatology, Palaeoecology* **237**, 293–304 (2006).
31. Martino, R. L. & Sanderson, D. D. Fourier and autocorrelation analysis of estuarine tidal rhythmites, lower Breathitt Formation (Pennsylvanian), eastern Kentucky, USA. *Journal of Sedimentary Research* **63**, 105–119 (1993).
32. Wentworth, C. K. A scale of grade and class terms for clastic sediments. *The Journal of Geology*, 377–392 (1922).
33. Hughen, B. K., McCormac, G., van der Plicht, J. & Spurk, M. INTCAL98 radiocarbon age calibration, 24,000–0 cal BP. *Radiocarbon* **40**, 1041–1083 (1998).
34. Passega, R. Texture as characteristic of clastic deposition. *AAPG Bulletin* **41**, 1952–1984 (1957).
35. Passega, R. & Byramjee, R. GRAIN-SIZE IMAGE OF CLASTIC DEPOSITS. *Sedimentology* **13**, 233–252 (1969).
36. Liu, Z. S., Zhao, H. T., Fan, S. Q. & Chen, S. Q. *Geology of the East China Sea* (in Chinese). Beijing: Science Press (2002).
37. Qin, Y. S., Zhao, Y. Y., Chen, L. R. & Zhao, S. L. *Geology of the East China Sea* (in Chinese). Science Press, Beijing (1987).

## Acknowledgements

We thank Dr. Paul Blanchon, who is at Institute of Marine Sciences and Limnology, National University of México, for giving highly constructive suggestions for the first manuscript. This work was sponsored by National Science Foundation of China (No. 41273110) and the China Postdoctoral Special Science Foundation (No. 200801440).

## Author contributions

Xiao, S. B. carried out grain-size analysis and prepared the primary manuscript. Li, R. prepared the figures. All authors reviewed and discussed the manuscript.

## Additional information

**Competing financial interests:** The authors declare no competing financial interests.

**License:** This work is licensed under a Creative Commons Attribution-NonCommercial-NoDerivs 3.0 Unported License. To view a copy of this license, visit <http://creativecommons.org/licenses/by-nc-nd/3.0/>

**How to cite this article:** Xiao, S., Li, R. & Chen, M. Detecting Sedimentary Cycles using Autocorrelation of Grain size. *Sci. Rep.* **3**, 1653; DOI:10.1038/srep01653 (2013).